Breast Cancer Res Treat (2015) 153:285–297
DOI 10.1007/s10549-015-3536-7

PRECLINICAL STUDY

TMEM33: a new stress-inducible endoplasmic reticulum transmembrane protein and modulator of the unfolded protein response signaling

Isamu Sakabe[1] · Rong Hu[1] · Lu Jin[1] · Robert Clarke[1] · Usha N. Kasid[1]

Received: 6 June 2015 / Accepted: 7 August 2015 / Published online: 13 August 2015

Abstract Endoplasmic reticulum (ER) stress leads to activation of the unfolded protein response (UPR) signaling cascade and induction of an apoptotic cell death, autophagy, oncogenesis, metastasis, and/or resistance to cancer therapies. Mechanisms underlying regulation of ER transmembrane proteins PERK, IRE1α, and ATF6α/β, and how the balance of these activities determines outcome of the activated UPR, remain largely unclear. Here, we report a novel molecule transmembrane protein 33 (TMEM33) and its actions in UPR signaling. Immunoblotting and northern blot hybridization assays were used to determine the effects of ER stress on TMEM33 expression levels in various cell lines. Transient transfections, immunofluorescence, subcellular fractionation, immunoprecipitation, and immunoblotting were used to study the subcellular localization of TMEM33, the binding partners of TMEM33, and the expression of downstream effectors of PERK and IRE1α. Our data demonstrate that TMEM33 is a unique ER stress-inducible and ER transmembrane molecule, and a new binding partner of PERK. Exogenous expression of TMEM33 led to increased expression of p-eIF2α and p-IRE1α and their known downstream effectors, ATF4-CHOP and XBP1-S, respectively, in breast cancer cells. TMEM33 overexpression also correlated with increased expression of apoptotic signals including cleaved caspase-7 and cleaved PARP, and an autophagosome protein LC3II, and reduced expression of the autophagy marker p62. TMEM33 is a novel regulator of the PERK-eIE2α-ATF4 and IRE1-XBP1 axes of the UPR signaling. Therefore, TMEM33 may function as a determinant of the ER stress-responsive events in cancer cells.

Keywords TMEM33 · Endoplasmic reticulum stress and unfolded protein response · PERK · IRE1α · Caspase-7 · Autophagy · Breast cancer

Abbreviations

ATF4	Activating transcription factor 4
ATF6	Activating transcription factor 6
ATF6f/c	Cytosolic domain of ATF6
CHOP	C/EBP(CCAAT/enhancer-binding protein) homologous protein
eIF2α	Eukaryotic translation initiation factor 2α
ER	Endoplasmic reticulum
GRP78/BiP	Glucose-regulated protein 78
IRE1α	Inositol-requiring enzyme 1α
LC3II	Microtubule-associated protein 1 light chain 3
PERK	Protein kinase RNA-like ER kinase
TG	Thapsigargin
TMEM33	Transmembrane protein 33
TN	Tunicamycin
UPR	Unfolded protein response
XBP1	X-box binding protein 1
XBP1-S	Active (spliced) XBP1

Electronic supplementary material The online version of this article (doi:10.1007/s10549-015-3536-7) contains supplementary material, which is available to authorized users.

✉ Usha N. Kasid
kasidu@georgetown.edu

[1] Georgetown Lombardi Comprehensive Cancer Center and Georgetown University Medical Center, Washington, DC, USA

Introduction

The endoplasmic reticulum (ER) is involved in several fundamental cellular processes including synthesis and sorting of secretory and membrane proteins, detoxification, and intracellular calcium homeostasis [1]. Correct folding of proteins in the ER lumen is regulated by folding and oxidizing enzymes in the presence of chaperones and glycosylating enzymes dependent on ATP and high Ca2+ levels. Misfolded proteins are exported to the cytoplasm for proteosomal degradation by a process known as the ER-associated degradation (ERAD) [2]. ER stress, as defined by the accumulation of misfolded or unfolded proteins above the threshold levels in the ER lumen, leads to activation of an ER-to-nucleus unfolded protein response (UPR) signaling cascade. The ER transmembrane proteins protein kinase RNA-like ER kinase (PERK), inositol-requiring enzyme 1α (IRE1α) and activating transcription factor 6 (ATF6α/β) sense ER stress, each then regulating one of the three distinct axes of the UPR signaling cascade [3]. ER stress-activated PERK phosphorylates serine 51 of eukaryotic translation initiation factor 2α (eIF2α), followed by the suppression of protein synthesis and a selective increase in ATF4 activity. Downstream effectors of PERK signaling include both pro-survival factors such as the transcription factor NRF2 and microRNA miR-211, which are associated with adaptation response, and pro-apoptotic factors including CHOP that can induce cell death [4, 5]. Stress-induced phosphorylation and activation of IRE1α results in activation of the transcription factor X-box binding protein 1 (XBP1) and increased expression of ER chaperones such as GRP78/BiP which, in turn, increase protein folding capacity in the ER lumen. Activated IRE1α also reduces protein load in the ER lumen by cleaving mRNAs encoding secretory and membrane proteins through regulated IRE1α-dependent decay (RIDD). In the ATF6α/β arm of the UPR signaling, ATF6α/β is transported to the golgi where it undergoes cleavage; cleaved ATF6 (ATF6f/ATF6c) functions as a transcription factor for several ER chaperones.

Mechanisms underlying regulation of PERK, IRE1α, and ATF6α/β, and how the balance of these activities determine outcome of the activated UPR, remain largely unclear. Indeed, depending on the acute or chronic ER stress and cellular context, activation of the UPR may lead to apoptotic cell death, senescence, autophagy, oncogenesis, metastasis, and/or resistance to chemotherapeutics and endocrines [6–14]. Identification of new molecules regulating UPR signals may advance understanding of the mechanistic and functional significance of UPR in cancer biology and therapy.

Here, we report characterization of transmembrane protein 33, TMEM33 (also known as SHINC-3) as a novel ER stress-inducible and ER transmembrane molecule and regulator of two main drivers of the UPR: PERK and IRE1α. Our data show that TMEM33 is a new binding partner of PERK. TMEM33 overexpression led to increased expression levels of both p-eIF2α and p-IRE1α and of their respective downstream effectors, ATF4 and XBP1-S in breast cancer cells. TMEM33 overexpression also led to increased expression of CHOP, cleaved caspase-7, and the autophagosome marker LC3II in these cells. Collectively, this work provides new mechanistic insights into the regulation of PERK and IRE1α signaling pathways via TMEM33 in cancer cells.

Materials and methods

Antibodies, reagents, and chemicals

Rabbit polyclonal antibody was custom generated against a TMEM33-specific peptide, KKVLDARGSNSLPLLR (amino acids 127–143; Covance Research Products Inc., Denver, PA). Polyclonal anti-GAPDH antibody (2275-PC-1) was purchased from Trevigen (Gaithersburg, MD, USA). Monoclonal anti-α-tubulin antibody (TU-02), monoclonal anti-Myc antibody (9E10), monoclonal horseradish peroxidase-conjugated anti-cMyc antibody (9E10HRP), polyclonal anti-PERK antibody (H-300), polyclonal anti-GRP78/BiP antibody (C-20), polyclonal anti-IRE1 antibody (H-190), polyclonal anti-Calnexin antibody (C-20), monoclonal anti-PARP antibody (F-2), polyclonal anti-ATF4 antibody (H-290), polyclonal anti-ATF-6α antibody (H-280), monoclonal anti-Cyclin D1 antibody (sc-20044); polyclonal anti-β-actin antibody (sc-1616) and Protein A/G PLUS-Agarose immunoprecipitation reagent were all purchased from Santa Cruz Biotechnology (Santa Cruz, CA, USA). Monoclonal anti-COX4 antibody (12C4) was obtained from Molecular Probes (Carlsbad, CA, USA). Monoclonal anti-Myc antibody (2276), monoclonal anti-PERK antibody (5683), polyclonal anti-phospho-eIF2α (Ser51) antibody (9721), polyclonal anti-eIF2α antibody (9722), monoclonal anti-phospho-eIF2α antibody (3597), monoclonal anti-ATF4 antibody (11815), monoclonal anti-LC3II antibody (12741), monoclonal anti-CHOP antibody (2895), polyclonal anti-cleaved-caspase-7 antibody (9491), polyclonal anti-caspase-7 antibody, and polyclonal anti-cleaved PARP antibody were all purchased from Cell Signaling Technology, Inc. (Beverly, MA, USA). Additional antibodies and reagents used were as follows: monoclonal anti-ATF6 antibody (IMG-273, Imagnex); polyclonal anti-XBP1 antibody (GWB-BACB31, Genway); polyclonal anti-phospho-IRE1α antibody (PA1-16927, Thermoscientific); monoclonal anti-p62 antibody (610832, BD-Bioscience);

FITC-conjugated monoclonal anti-Calnexin antibody (BD Transduction Laboratories); horseradish peroxidase-conjugated mouse and rabbit secondary antibodies (Amersham Pharmacia Biotech, Piscataway, NJ, USA); Lipofectamine 2000, Lipofectamine LTX, and Lipofectin (Invitrogen Life Technologies, Carlsbad, CA, USA); Fu Gene HD (Roche); proteinase inhibitor cocktail tablets (Roche Diagnostics, Indianapolis, IN, USA); ECL Plus Western blotting detection system (Amersham Biosciences); Coomassie protein assay reagent and Surfact-Amps NP-40 (Pierce Biotechnology, Inc., Rockford, IL, USA); Tween 20 (Bio-Rad Laboratories, Inc., Hercules,CA, USA); Re-Blot plus mild antibody stripping solution (Chemicon International, Inc., Temecula, CA, USA); Restore Western blot stripping buffer (21059, ThermoScientific), and thapsigargin, tunicamycin from Streptomyces sp., dimethyl sulphoxide Hybri-Max Sterile filtered (DMSO), and etoposide (Sigma-Aldrich, St. Louis, MO, USA).

Cell lines and cultures

MCF-7 human breast cancer cells were obtained from the American Type Culture Collection (Rockville, MD, USA) and Tissue Culture Shared Resource of the Georgetown Lombardi Comprehensive Cancer Center. HEK293T human embryonic kidney cells were obtained from the American Type Culture Collection (Rockville, MD, USA). Human prostate cancer cells (PC-3 and DU-145), breast cancer cells (MDA-MB231), HeLa, and COS-1 cells were obtained from the Tissue Culture Shared Resource of the Georgetown Lombardi Comprehensive Cancer Center. All cell lines were grown as monolayers in Dulbecco's Modified Eagle Medium (DMEM) (Invitrogen Life Technologies, Carlsbad, CA, USA) supplemented with 5 or 10 % heat-inactivated fetal bovine serum. Endocrine-sensitive (LCC1) and endocrine-resistant breast cancer cells (LCC9), and antiestrogen-resistant MCF-7 cells (MCF7RR) were obtained and established as reported earlier [15–17]. LCC1, LCC9, and MCF7RR cells were maintained in IMEM without phenol red and supplemented with 5 % charcoal-stripped calf serum (CCS). All cell cultures were maintained at 37 °C under 95 % relative humidity and 95 % O_2:5 % CO_2 atmosphere.

Construction of *Myc-TMEM33* expression vector

TMEM33 cDNA (741 bp) was amplified by RT-PCR using total mRNA from human testes (Ambion, Foster City, CA) and cloned into the pCR2.1 vector (Invitrogen). N-terminal Myc-tagged TMEM33 ORF (771 bp) was amplified by PCR using *TMEM33* in pCR2.1 as template. The forward primer sequence containing the translation initiation codon, the Myc epitope (*underlined*), and Bgl II primer (bold) was 5′-G**AGATCT**GCCATGGAGCAGAAACTCATCTCTGAAGAGGACCTGATGGCAGATACGACCCCGAAC-3′, and the reverse primer sequence containing the MulI primer (bold) was 5′-G**ACGCGT**CTATGGAACTGTTGGTGCC -3′ as described earlier [18]. The PCR conditions were as follows: 95 °C for 4 min; 40 cycles of denaturation at 94 °C for 30 s; annealing at 65 °C for 1 min; extension at 72 °C for 1 min; and a final extension at 72 °C for 5 min. The amplified product was subjected to electrophoresis in 1 % agarose gels and cloned into the pCR3.1 expression vector. *TMEM33* cDNA sequence was verified by automated DNA sequencing of both strands using vector-based forward and reverse primers as detailed earlier [18, 19].

Transient cDNA transfections

COS-1, HEK-293T, and PC-3 prostate cancer cells were transiently transfected using Lipofectamine 2000 (Invitrogen, Carlsbad, CA). HeLa cells were transiently transfected using FuGene HD (Roche), and MCF-7 and MDA-MB231 breast cancer cells were transiently transfected using Lipofectamine LTX (Invitrogen) as described in Supplementary Materials and methods.

Immunofluorescence and immunostaining

COS-1 cells were grown overnight on coverslips placed in a six well plate, one coverslip/well. Approximately, 3×10^4 cells were seeded/well. Next day, cells were transfected with 1 μg of *Myc-TMEM33* or empty vector using Lipofectamine 2000. Forty eight hours post-transfection, the medium was removed and cells were immediately fixed in 3.7 % paraformaldehyde, followed by immunofluorescence and immunostaining using various antibodies as described in Supplementary Materials and methods.

Subcellular fractionation

Approximately, 5×10^6 MCF-7 cells were seeded per 150 mm tissue culture dish. Next day, the cells were collected by trypsinization and washed once with ice-cold phosphate-buffered saline (PBS). The cytosolic, mitochondrial (heavy membrane), microsomal (light membrane), and nuclear fractions were isolated as described in Supplementary Materials and methods.

Immunoprecipitation and immunoblotting

The whole cell lysate (approximately 2 mg protein) was incubated with 25 μL of agarose-conjugated anti-Myc antibody on a rotator at 4 °C overnight. The antibody-conjugated agarose beads were washed 1x in cell lysis

buffer and used for immunoblotting as reported earlier [20] and detailed in Supplementary Materials and methods.

Thapsigargin and tunicamycin treatments

Stock solutions of thapsigargin (TG, 2 mM) and tunicamycin (TU, 2 mg/mL) were made in DMSO and stored at −20 °C. Cells from approximately 80 % confluent monolayers were used. The culture medium was removed and fresh DMEM containing 10 % FBS and the desired final concentration of TG or TU was added to the cells and incubation continued for various periods, followed by cell lysis and Western blotting as described in Supplementary Materials and methods.

Results

TMEM33 is a novel endoplasmic reticulum transmembrane protein

We identified TMEM33 as a novel cDNA fragment (191 bp) in a differentially displayed mRNA screen of cancer cells treated with antisense *raf* oligonucleotide or control mismatch oligonucleotide [GenBank accession number AF403224]. Subsequent sequential homology search of the human expressed sequence tag (EST) database [21] led to identification of the full-length *TMEM33* cDNA sequence (7717 bp) as shown in Fig. 1a. The longest open reading frame of the full-length *TMEM33* cDNA encodes a new 247 amino acids (aa) protein (approximately 28 kDa M_r) (Fig. 1b, Supplementary Fig. 1). The TMEM33 amino acid sequence revealed three transmembrane helices (32–52 aa, 101–121 aa, and 156–176 aa), at least one phosphorylation site (T65) and two ubiquitination sites (K148 and K221) [22–24] (Fig. 1b). Using northern hybridization, four major *TMEM33* transcripts (7.7, 4.0, 2.5, and 1.5 kb) were detected in most normal human tissues and cancer cell lines tested (Fig. 2).

Based on prediction of its likely subcellular localization, the TMEM33 protein appeared to be localized to ER [25]. Subcellular localization of TMEM33 was demonstrated using a combination of immunofluorescence and biochemical fractionation analyses. COS-1 cells were transiently transfected with either a Myc epitope-tagged *TMEM33* expression vector (*Myc-TMEM33*) or empty vector. Immunofluorescence staining showed co-localization of *Myc-TMEM33* with Calnexin and ER-tracker but not mito-tracker or WGA staining (Fig. 3a). Expression of *Myc-TMEM33* in COS-1 transfectants was verified by immunoblotting (Fig. 3b).

Subcellular localization of the endogenous TMEM33 protein was examined by cell fractionation and immunoblotting using a custom-generated rabbit polyclonal antibody against a TMEM33-specific epitope (aa 127–143). The anti-TMEM33 antibody recognized an approximately 28 kDa protein in human prostate cancer cells (PC-3 and DU-145); pre-immune serum had no immune reactivity at the corresponding location (Supplementary Fig. 2a). The anti-TMEM33 antibody was further validated by sequential immunoblotting of cell lysates from COS-1 *Myc-TMEM33* transfectants with anti-Myc and anti-TMEM33 antibodies. These two antibodies recognized an overlapping band at ∼28 kDa in COS-1 transfectants (Supplementary Fig. 2b). Using the custom-generated anti-TMEM33 antibody, human endogenous TMEM33 (∼28 kDa) was detected in several human cancer cell lines including A549, Aspc-1, Colo-357, MDA-MB435, MCF-7, and HeLa cells (data not shown). In the combined cell fractionation and immunoblotting assay, Calnexin was detected in both the heavy membrane pellet (HM) and the ER-containing microsomal fractions (MS) of MCF-7 cells; heavy membrane pellets contain mitochondrial, lysosomal, and ER-resident proteins. Similar to Calnexin, endogenous TMEM33 expression was seen in both the HM and MS fractions of MCF-7 cells but not in the nuclear or cytosolic fractions (Fig. 3c). Together with the predicted 2D topology of TMEM33 [26, 27] (Fig. 3d) these data establish TMEM33 as a novel ER transmembrane resident protein.

TMEM33 is an ER stress-inducible molecule

The ER localization of TMEM33 prompted us to ask whether TMEM33 expression is stimulated in response to known inducers of ER stress including thapsigargin (TG), an inhibitor of ER Ca^{2+} ATPase, tunicamycin (TU), an inhibitor of N-linked glycosylation, and low glucose. Expression of TMEM33 was analyzed in HeLa cells exposed to TG, TU or low glucose. TMEM33 protein expression was increased in response to ER stress (Fig. 4a, b). Consistent with these observations, a significant induction of the largest *TMEM33* transcript (7.7 kb) was seen in HeLa cells treated with thapsigargin (Fig. 4c). As expected, GRP78/BiP, a well-known ER stress-inducible protein chaperone in the ER lumen, was also induced in HeLa cells under similar conditions (data not shown). In addition, ER stress-inducible expression of TMEM33 and GRP78/BiP was also noted in PC-3 prostate cancer cells (data not shown). Thus, TMEM33 is a new ER stress-inducible protein.

TMEM33 overexpression is associated with enhanced stimulation of the ER stress-responsive PERK/p-eIF2α/ATF4 signaling pathway

To determine whether TMEM33 is a component of the ER stress-inducible UPR signaling pathway, we first looked for

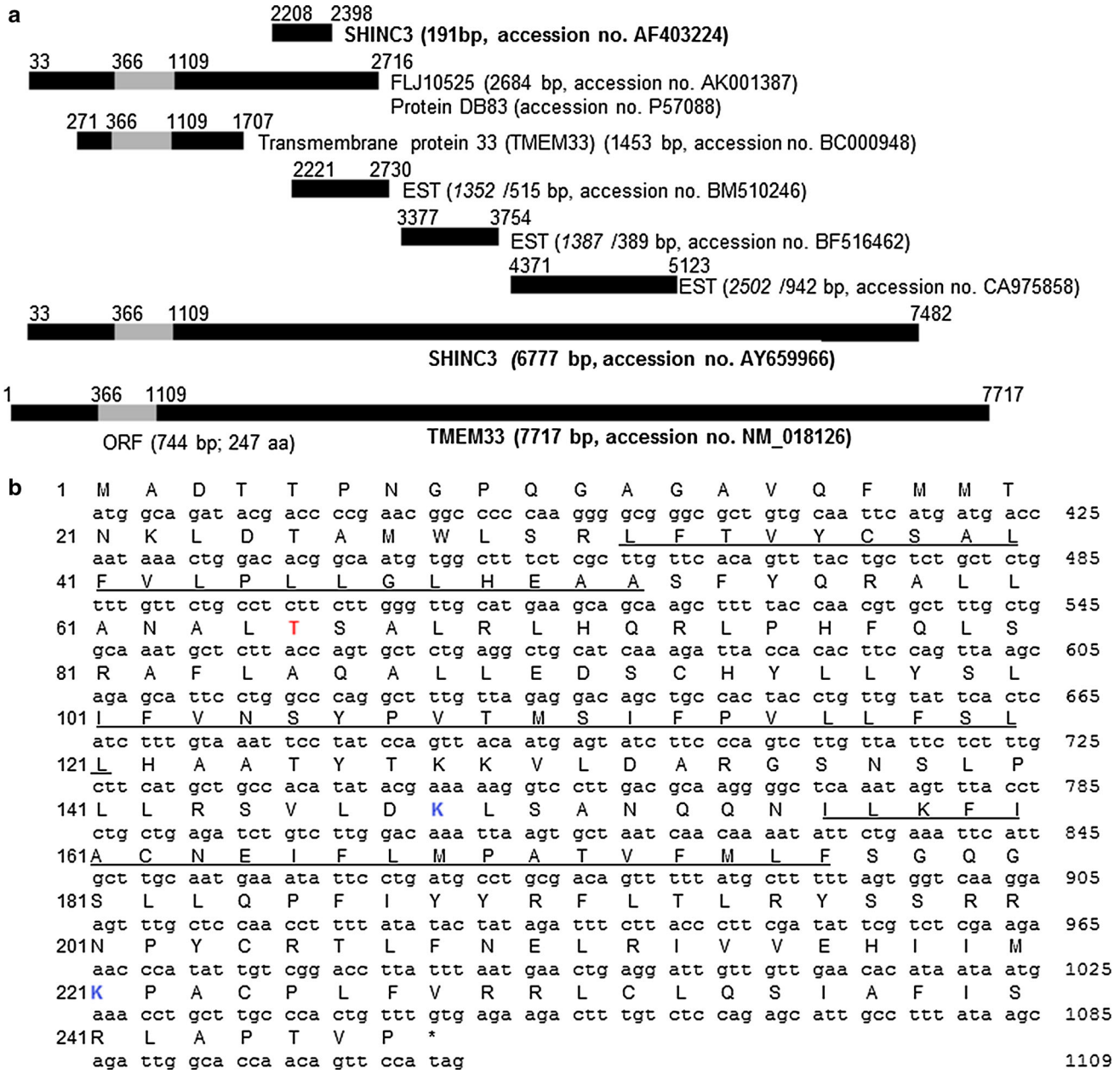

Fig. 1 Schematic maps of *TMEM33* cDNA, and predicted open reading frame and amino acid sequence of TMEM33. **a** Maps of the complete human *TMEM33 (alias SHINC3)* cDNA and overlapping partial clones are shown. The gray box represents the coding region and the black boxes represent the 5′- and 3′- untranslated regions of the cDNA sequence. *Italicized* numbers represent the original lengths of the overlapping clones in the GenBank database. The NCBI BLAST program [43] was used to identify the overlapping sequences and deduce the full-length sequence of *TMEM33* cDNA. **b** Predicted open reading frame (366–1109 bp) and amino acid sequence alignment of TMEM33 protein (247 aa). Locations of three transmembrane helices (32–52 aa, 101–121 aa, and 156–176 aa, *underlined*), a phosphorylation site (T65, *red*) and two ubiquitination sites (K148 and K221, *blue*) are shown

interaction(s) between TMEM33 and the ER membrane-resident molecules PERK, IRE1α, and ATF6. HEK293T cells were transiently transfected with the *Myc-TMEM33* plasmid and treated with 1 μM TG for various times. Using a reciprocal co-immunoprecipitation assay, our findings show an ER stress-related interaction between TMEM33 and PERK (Fig. 5a). Myc-TMEM33 did not interact with either IRE1α or ATF6 under similar conditions (data not shown). Next, we examined the effects of TMEM33 overexpression on downstream effectors of activated PERK (p-eIF2α; ATF4). As shown in Fig. 5b and c, and Supplementary Fig. 3, overexpression of TMEM33 was associated with enhanced basal and ER stress-induced expression of p-eIF2α and ATF4 in *Myc-TMEM33*

transfectants, relative to empty vector control transfected HEK293T cells. These data establish TMEM33 as a novel binding partner of PERK and demonstrate that TMEM33 overexpression correlates with enhanced activation of the ER stress-inducible PERK/p-eIF2α/ATF4 signaling.

TMEM33 overexpression and increased expression of ER stress-induced cell death signals

We next determined the effects of TMEM33 overexpression on various cell death signals. HeLa cells were transiently transfected with a *Myc-TMEM33* or control vector and exposed to TG (1 μM) for indicated times, followed by immunoblotting of whole cell lysates with various antibodies (Fig. 6). For quantification of relative levels of cleaved caspase 9, cleaved caspase 7 and cleaved PARP in *Myc-TMEM33* transfectants versus control vector, expression levels were first normalized against α-Tubulin in corresponding lanes. The fold Δ in relative expression level in Myc-TMEM33 cells was calculated by dividing normalized value in *Myc-TMEM* 33 transfectants by normalized value in *pCR3.1* transfectants in the corresponding treatment group. Basal levels of cleaved caspase 9 were found to be higher in *Myc-TMEM33* transfected HeLa cells relative to control vector transfectants (*Myc-TMEM33* versus *pCR3.1*, Cl. Caspase 9, untreated (UT), 1.8 fold). Increased expression levels of cleaved caspase 7 and cleaved PARP were observed in *Myc-TMEM33* transfectant HeLa cells following TG treatment relative to control vector transfectants (*Myc-TMEM33* versus *pCR3.1:* Cl. Caspase 7, TG (1 μM, 48 h), 5.0 fold; Cl. PARP, TG (1 μM, 48 h), 3.0 fold). Increased expression levels of cleaved Caspase 7 and cleaved PARP were also observed following TG treatment of COS-1 cells transiently transfected with *Myc-TMEM33* versus control vector transfectants (Supplementary Fig. 4a). In addition, Caspase 2 expression was found to be increased in *Myc-TMEM33* transfectant COS-1 cells versus control transfectants (Supplementary Fig. 4a). Interestingly, expression of cleaved caspase 3 did not seem to change in these cells (data not shown). Furthermore, constitutive expression of cleaved caspase 7 was also seen in *TMEM33*-transfected

Fig. 3 TMEM33 is an ER transmembrane resident protein. **a** Immunofluorescence analysis of ER localization of TMEM33 in COS-1 transfectants. After 48 h of transfection with *Myc-TMEM33* cDNA expression vector, COS-1 transfectants were fixed and immunostained as described in "Materials and methods" section. For ER-tracker or Mito-tracker staining, transfected cells were first incubated with these dyes. Right subpanels: *a* DAPI; *d* anti- Calnexin antibody; *g* ER-tracker; *j* Mito-tracker; *m*, WGA. *Middle subpanels* (*b*, *e*, *h*, *k*, *n*): anti-Myc antibody. *Left panels* (*c*, *f*, *i*, *l*, *o*): merge of corresponding right and middle panels. **b** Expression of Myc-TMEM33 protein in transiently transfected COS-1 cells was confirmed by immunoblotting with anti-Myc antibody. The blot was reprobed with anti-GAPDH antibody. *UT* untransfected. **c** The subcellular localization of endogenous TMEM33. MCF-7 cells were homogenized and fractionated into nuclear, heavy membrane (HM), microsomal (MS), and cytosolic fractions, followed by sequentially immunoblotting of the cell fractions using anti-TMEM33, anti-Calnexin (ER membrane), anti-PARP (nucleus), anti-COX4 (mitochondria), and anti-tubulin (cytosol) antibodies. WCE, whole cell extract**. d** The ER membrane structure of TMEM33. TOPO2, transmembrane protein display software, was used to display 2D topology of TMEM33. ER lumen, N-terminus 1–31 aa; 122–155 aa; ER membrane, 32–52 aa; 101–121 aa; 156–176 aa; Cytoplasm, 53–100 aa; 177–247 aa—C terminus; Potential phosphorylation site (T65) (*red*) and two ubiquitination sites (K148 and K221) (*blue*) are shown

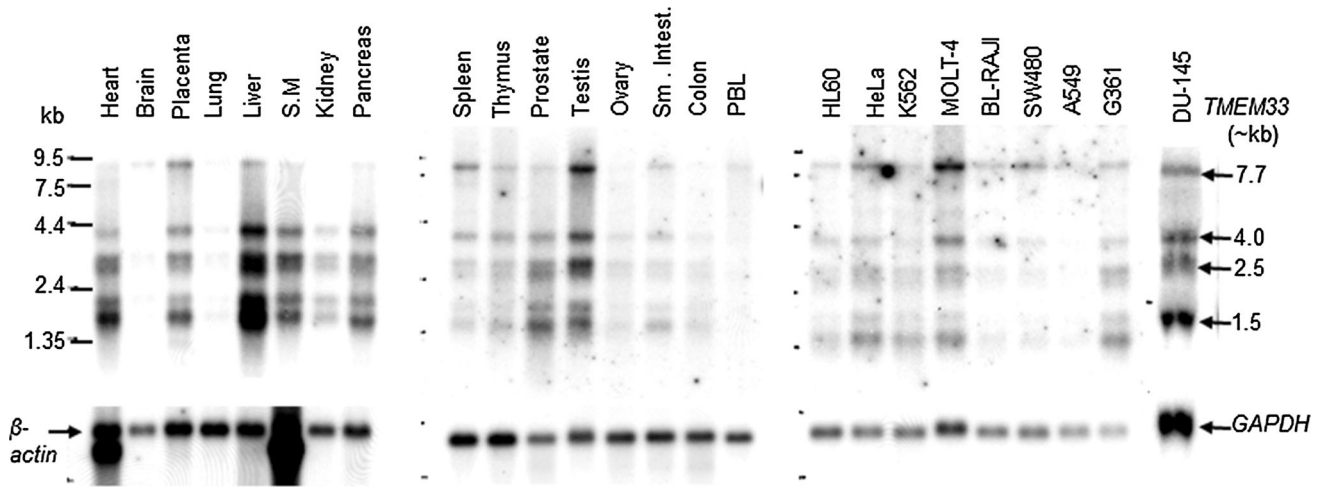

Fig. 2 Expression analyses of *TMEM33* transcripts in normal human tissues and human cancer cell lines. The mRNA blots (Clontech) were sequentially probed with a radiolabeled *TMEM33* cDNA probe, followed by *β-actin* or *GAPDH* cDNA probe. S.M., smooth muscle; PBL, peripheral blood lymphocytes; HL-60, promyelogenous leukemia; K-562, chronic myelogenous leukemia; MOLT-4, lymphoblastic leukemia; BL-Raji, Burkitt's lymphoma; SW480, colorectal adenocarcinoma; A549, lung carcinoma; G361, melanoma; DU-145, prostate cancer

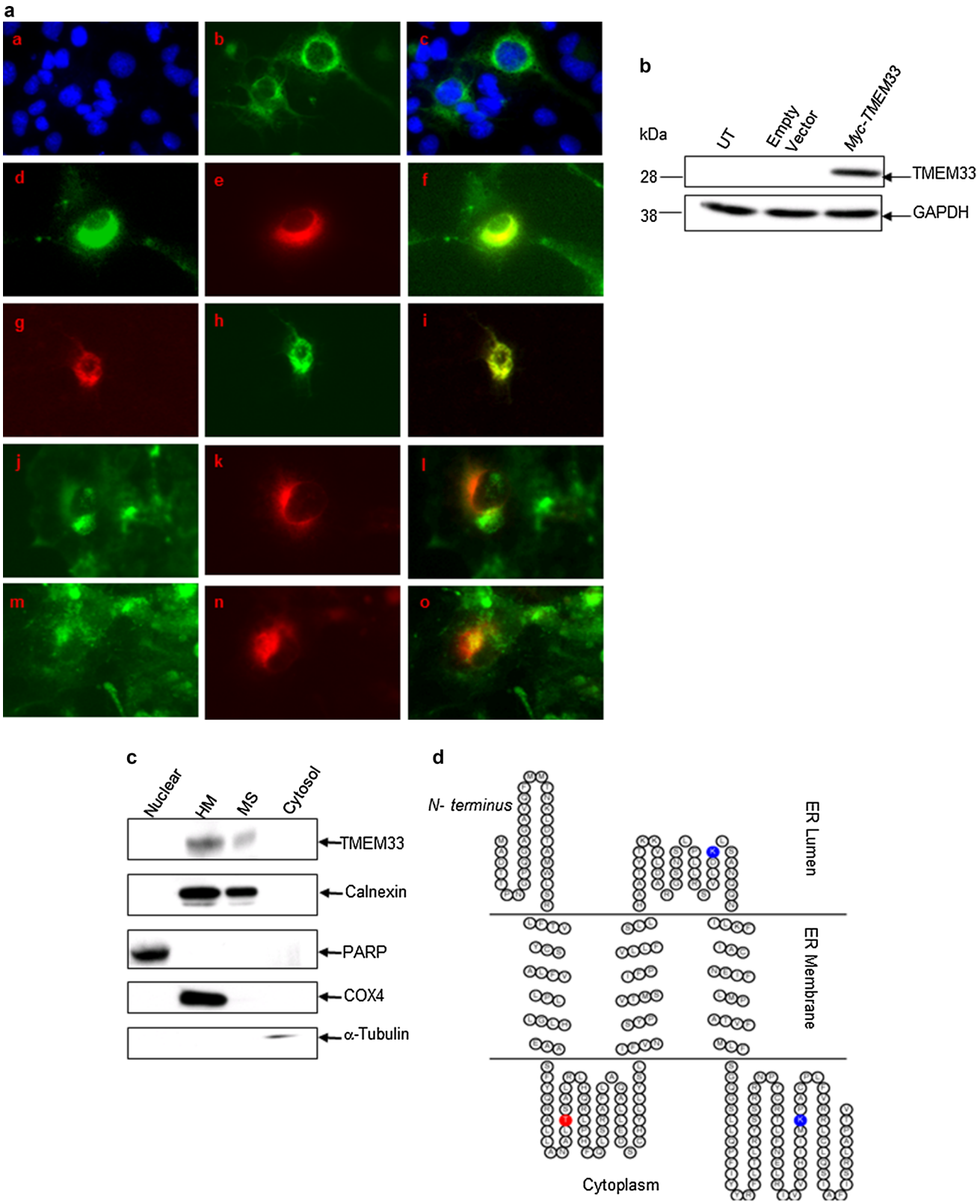
a
a
b
c
d
e
f
g
h
i
j
k
l
m
n
o
b
kDa
UT
Empty Vector
Myc-TMEM33
28
38
TMEM33
GAPDH
c
Nuclear
HM
MS
Cytosol
TMEM33
Calnexin
PARP
COX4
α-Tubulin
d
N- terminus
ER Lumen
ER Membrane
Cytoplasm

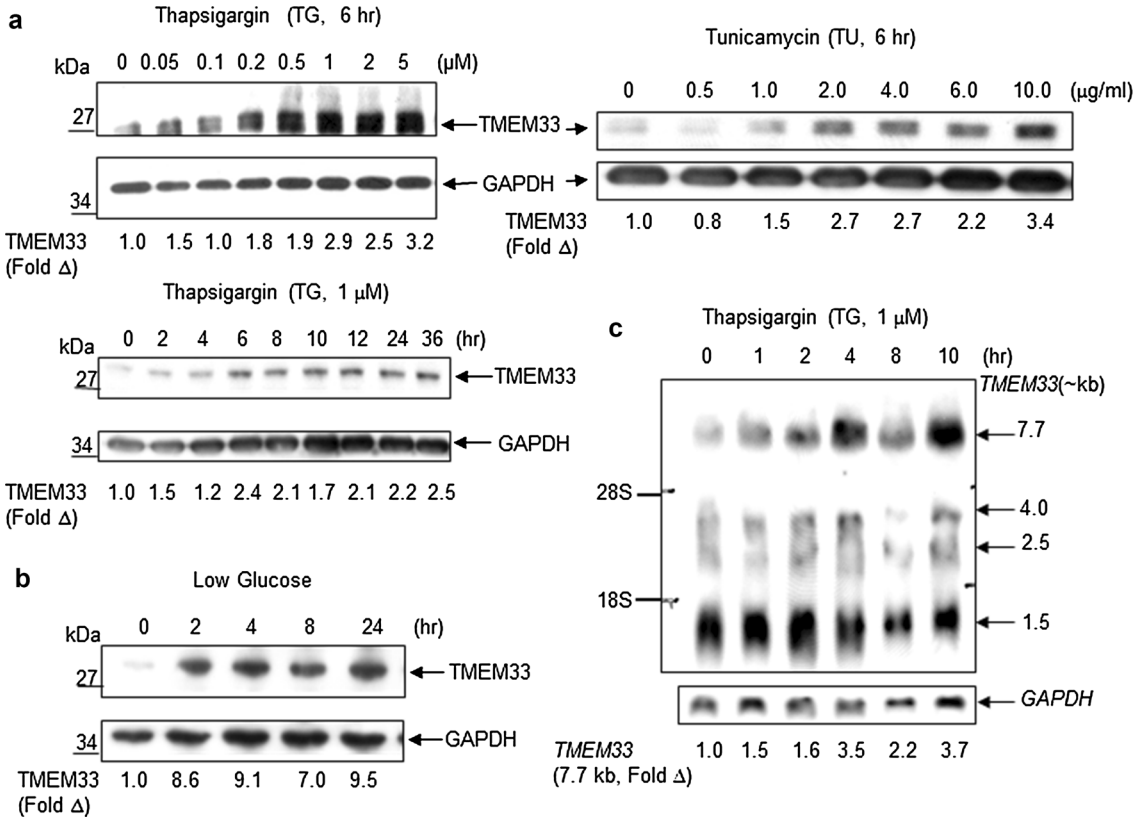

Fig. 4 TMEM33 is an ER stress-inducible molecule. **a** HeLa cells were treated with indicated doses of thapsigargin (TG) or tunicamycin (TU) for various times, followed by immunoblotting with anti-TMEM33 antibody. The blots were reprobed with anti-GAPDH antibody. The expression levels of TMEM33 were quantified using ImageQuant software (Molecular Dynamics), and normalized against GAPDH in corresponding lanes. The fold *open triangle* indicates TMEM33 level at various doses or time points relative to control lane. Data shown are representative of two to three independent experiments. **b** HeLa cells were grown in high glucose (25 mM) DMEM containing 10 % FBS. The medium was switched to low glucose (5.5 mM) DMEM containing 10 % FBS for the times indicated, followed by sequential immunoblotting with anti-TMEM33 antibody and anti-GAPDH antibody. Normalized expression levels of TMEM33 were quantified as in *panel a*. Data shown are representative of two independent experiments. **c** Northern blot analysis of *TMEM33* mRNA in HeLa cells treated with thapsigargin as shown. The blot was reprobed with radiolabeled *GAPDH* cDNA. The normalized expression levels of 7.7 kb *TMEM33* transcript at various time points were quantified using ImageQuant software (Molecular Dynamics)

MCF-7 breast cancer cells but not in control pCR3.1-transfected cells (Fig. 7, Supplementary Fig. 4b).

TMEM33 overexpression and constitutive activation of the PERK-p-eIF1α-ATF4 and IRE1α-XBP1 axes of the UPR signaling and autophagy in breast cancer cells

To address the consequences of TMEM33 overexpression in human cancer cells, MCF-7 breast cancer cells were transiently transfected with either the *Myc-TMEM33* or pCR3.1 vector, followed by immunoblotting of the cell lysates with antibodies against various components of the UPR signaling pathways. Figure 7 shows that exogenous expression of TMEM33 was sufficient to increase basal levels of p-eIF2α, ATF4, CHOP, cleaved caspase 7, p-IRE1α, and XBP1-S but not cleaved ATF6. In addition, cyclin D1 expression, a marker of cell cycle progression and oncogenesis, was decreased in *Myc-TMEM33* transfectant MCF-7 cells. The latter observations seem to be inconsistent with data showing high TMEM33 expression in several tumor tissues including breast cancer (Supplementary Fig. 5). Moreover, *TMEM33* is reported to be amplified in approximately 10 % of breast cancer patient xenografts [28–30]. During autophagy, microtubule-associated protein-1 light chain 3 (LC3I) is converted to its membrane-bound form (LC3II). We have previously reported that overexpression of XBP1 can regulate autophagy through its control of BCL2 [31–33]. Increased expression of LC3II and decreased expression of p62/sequestosome 1 (SQSTM1), ubiquitin-binding protein and promoter of apoptosis, was detected in *Myc-TMEM33* transfected MCF-7 cells relative to controls (Fig. 7). Similar observations were made in hormone refractory MDA-

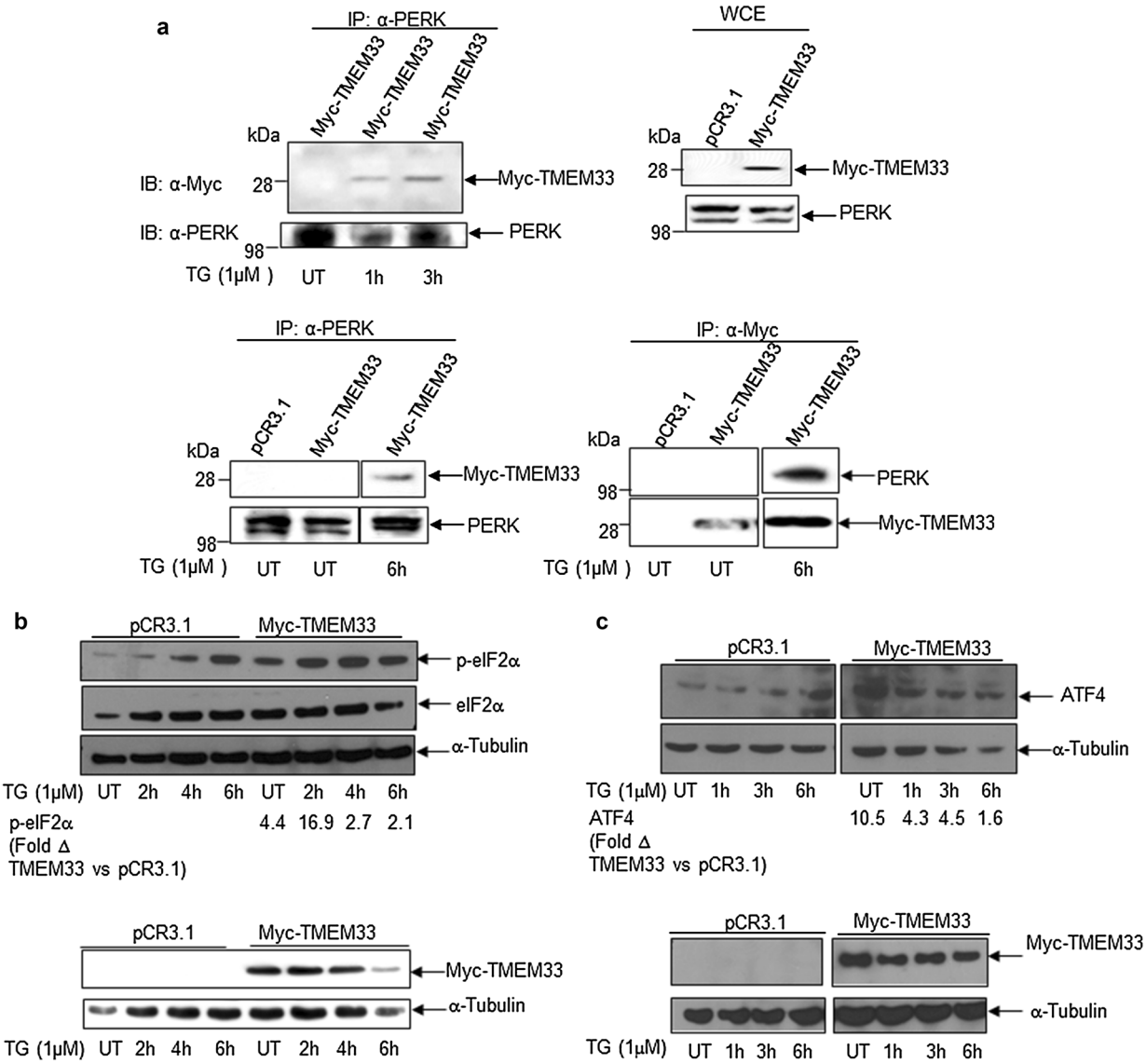

Fig. 5 TMEM33 is a binding partner of PERK and TMEM33 overexpression correlates with increased levels of basal and ER stress- induced p-elF2α and ATF4 expression. **a** TMEM33 interacts with PERK in the presence of ER stress. HEK293T cells were transiently transfected with *Myc-TMEM33* for 48 h at 37 °C, followed by treatment with 1 μM TG for the times indicated. The whole cell lysates were subjected to immunoprecipitation using anti-Myc antibody or anti-PERK antibody-conjugated Protein A/G and the immunoprecipitates were analyzed by Western blotting as indicated. Representative data from two independent experiments are shown. *IP* immunoprecipitation; *IB* immunoblotting; *WCE* whole cell extracts. *UT* untreated. **b** Increased basal and ER stress-induced expression of p-eIF2α in *Myc-TMEM33* transfected HEK293T cells. HEK293T cells were transiently transfected with *Myc-TMEM33* or *pCR3.1* (empty vector) and incubated for 48 h at 37 °C, followed by treatment with 1 μM TG as indicated. Whole cell lysates were analyzed by Western blotting with anti-p-eIF2α antibody. Blots were reprobed with anti- eIF2α and anti-α-Tubulin antibodies (*top panel*). Cell lysates were also probed with anti-Myc and anti-α-Tubulin antibodies (*bottom panel*). For quantification of relative p-eIF2α levels in *Myc-TMEM* transfectants versus control vector at various time points, first total eIF2α levels were normalized against α-Tubulin in corresponding lanes. Expression levels of p-eIF2α were then normalized against α-Tubulin-normalized eIF2α levels in corresponding lanes. The fold Δ in p-eIF2α level was calculated by dividing normalized p-eIF2α level in *Myc-TMEM* transfectants by normalized p-eIF2α level in *pCR3.1* transfectants in the corresponding treatment group. Representative data from three independent experiments are shown. UT, untreated. **c** Increased expression of ATF4 in *Myc-TMEM33* transfected HEK293T cells. Whole cell extracts of empty vector (*pCR3.1*) or *Myc-TMEM33* transfected cells were prepared after thapsigargin treatment (TG) as described in Materials and methods. Cell lysates were sequentially immunoblotted with anti-ATF4 and anti-α-Tubulin antibodies (*top panel*). Cell lysates were also probed with anti-Myc and anti-α-Tubulin antibodies (*bottom panel*). For quantification of relative ATF4 levels in *Myc-TMEM33* transfectants versus control vector at various time points, expression levels of ATF4 were normalized against α-Tubulin in corresponding lanes. The fold Δ in ATF4 level was calculated by dividing normalized ATF4 level in *Myc-TMEM33* transfectants by normalized ATF4 level in *pCR3.1* transfectants in the corresponding treatment group. Representative data from two independent experiments are shown. *UT* untreated

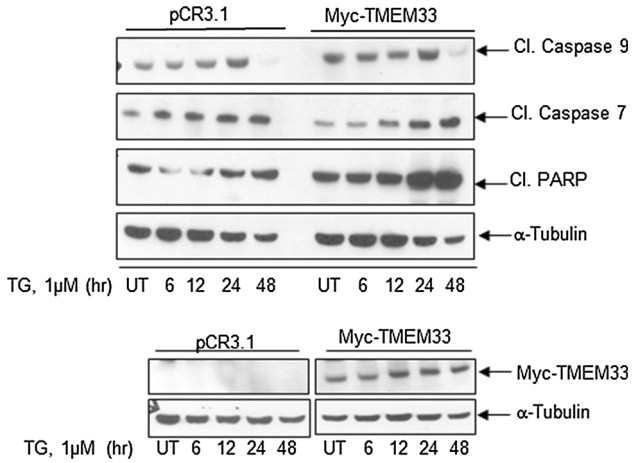

Fig. 6 TMEM33 overexpression is associated with increased ER stress-inducible expression of cleaved caspase 7 and cleaved PARP. HeLa cells were transiently transfected with *Myc-TMEM33* or *pCR3.1* (empty vector) and incubated for 48 h at 37 °C, followed by treatment with 1 μM TG for indicated times. Cell lysates were analyzed by western blotting for expression of pro-apoptotic signals. Blots were reprobed with anti-α-Tubulin antibody (*top panel*). Cell lysates were also probed with anti-Myc and anti-α-Tubulin antibodies (*bottom panel*). *UT* untreated

MB-231 breast cancer cells (Supplementary Fig. 6). Hence, TMEM33 overexpression is associated with constitutive activation of PERK-p-eIF1α-ATF4 and IRE1α-XBP1-S signaling and autophagy in breast cancer cells.

Discussion

This study is the first report of TMEM33 as a new ER stress-inducible and ER transmembrane resident molecule. PERK and IRE1α axes of the UPR play prominent roles in regulation of adaptation and cell death signals, yet how these two receptors are regulated remains unclear. Here, we demonstrate: (1) TMEM33 is a novel binding partner of PERK and that TMEM33 overexpression correlates with increased expression of downstream effectors of PERK, p-eIF2α, and ATF4, and cleaved caspase 7 in cells challenged with thapsigargin, (2) association of enhanced expression of TMEM33 with increases in components of the activated PERK and IRE1α signaling pathways (p-eIF2α, ATF4, CHOP, cleaved caspase 7, XBP1-S) in breast cancer cells, and (3) association of enhanced

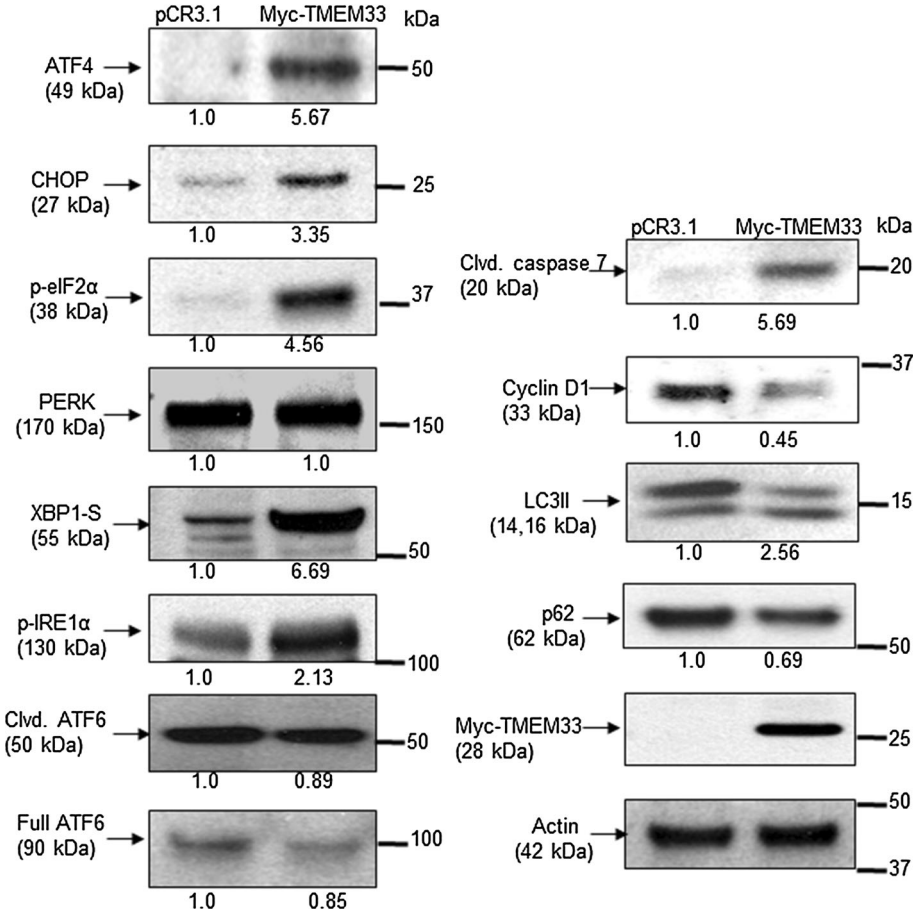

Fig. 7 Exogenous expression of TMEM33 in MCF-7 breast cancer cells is associated with constitutive activation of the PERK and IRE1α axes of the UPR signaling. MCF-7 cells were transiently transfected with *Myc-TMEM33* or pCR3.1 control vector. Adherent and floating cells were collected 24 h post-transfection. Cells were lysed in RIPA lysis buffer supplemented with protease inhibitor (Roche), 10 mM glycerophosphate, 1 mM sodium orthovanadate, 5 mM pyrophosphate, and 1 mM PMSF. Cell lysates (10 μg protein) were immunoblotted with indicated antibodies (all 1:1000 dilution)

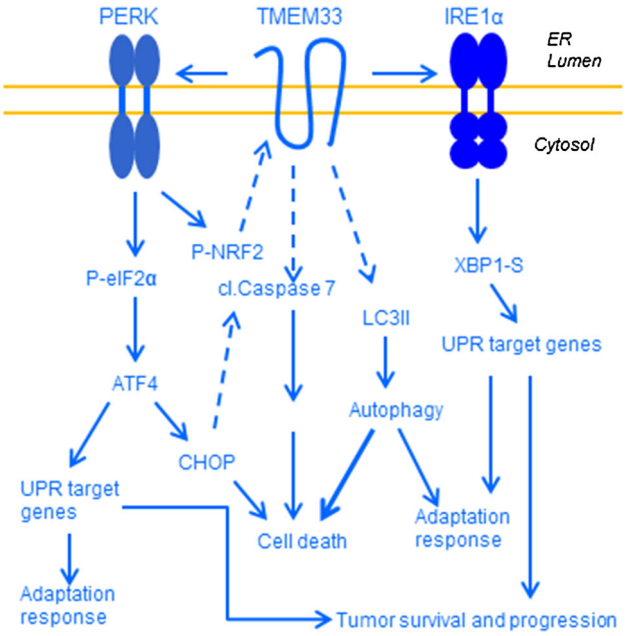

Fig. 8 Proposed model of a role of TMEM33 in regulation of the PERK and IRE1α axes of the unfolded protein response signaling. ER stress leads to increased expression of TMEM33 and activation of PERK resulting in enhanced levels of p-eIF2α and ATF4. Depending of the cell type, overexpression of TMEM33 may also increase expression of p-IRE1α and its effector XBP1-S. Additional downstream effectors include increased expression of CHOP, cleaved caspase-7, cleaved PARP, and autophagosome marker LC3II, and reduced expression of p62. *Dashed arrows* indicate as yet unknown pathways

expression of TMEM33 with increased autophagy in breast cancer cells. Autophagy has been associated with tumor cell resistance to various therapies. In pilot studies, we also tested whether TMEM33 may serve as a new prognostic marker in certain estrogen receptor-positive breast cancers. Gene expression microarrays were used to measure TMEM33 expression in endocrine-resistant (LCC9, MCF7RR) and sensitive breast cancer cells (LCC1 and MCF7) [15–17], and in clinical specimens [34–37]. TMEM33 mRNA expression was found to be higher in endocrine-resistant breast cancer cells as compared with their matched sensitive control cells. In addition, early recurrent breast cancer specimens showed high TMEM33 expression when compared with non-recurrent breast tumors (Supplementary Fig. 7). Taken together, our current observations suggest a working model where TMEM33 may function as a critical determinant of the balance between PERK and IRE1α-mediated apoptotic, adaptive and neoplastic transformation events in cancer cells (Fig. 8).

How TMEM33 expression is regulated remains unknown. The proximal promoter region of the *TMEM33* gene shows putative binding site for NRF-2, a prosurvival transcription factor downstream of the activated PERK (Supplementary Fig. 1c). It is tempting to speculate that an as yet unknown combination of feedback and cross-talk exists. For example, where ER stress activates PERK and increases TMEM33 expression via NRF-2, and increased TMEM33 overexpression, depending on the cell type, promotes PERK and IRE-1α activated signaling. TMEM33 may also interact with other proteins. At least one phosphorylation site (Thr 65) and two ubiquitination sites (Lys 148 and Lys 221) are predicted within the open reading frame of TMEM33 (Supplementary Fig. 1b). TMEM33 may be a member of the family of ubiquitin-modified proteins [38–40]. The STRING database [41] also predicts potential interaction of TMEM33 with ubiquitin C (UBC), and ubiquitin specific peptidase 19 (USP19), associated with ubiquitin-dependent proteolysis (Supplementary Fig. 8). TMEM33 may also interact with the retention in endoplasmic reticulum 1 protein (RER1), which is involved in the retrieval of ER membrane proteins from the early golgi compartment (Supplementary Fig. 8).

Present report supports the hypothesis that TMEM33 may function as a multi-faceted molecule in cancer cells. While our data suggest that TMEM33 overexpression correlates with enhanced expression of apoptotic signals (CHOP and cleaved caspase7), constitutive expression of TMEM33 was found to be high in a limited number of endocrine-resistant breast cancer cells and in early recurrent breast cancer specimens tested. The latter observations are consistent with the roles of PERK and ATF4 in tumor cell survival [42]. Moreover, autophagy may increase survival of tumor cells [8, 9]. We observed increased expression of autophagosome marker LC3II and down-regulation of p62/sequestosome 1 (SQSTM1) in breast cancer cells overexpressing TMEM33, suggesting induction and completion of autophagy. In conclusion, TMEM33 offers a new regulatory mechanism of the UPR and may serve as a determinant of the outcome of activated UPR signaling cascade.

Acknowledgments We thank Dr. Sona Vasudevan for analysis of *TMEM33* profiles in The Cancer Genome Atlas (TCGA) and cBioPortal databases. This work was funded by NIH Grants CA68322, CA74175, CA149147, and CA184902 and NeoPharm, Inc. Several cell lines were obtained from the Tissue Culture Shared Resource of the Georgetown Lombardi Cancer Center. The RNA array expression profiling was performed at the Genomics and Epigenomics Shared Resource and the immunofluorescence imaging was performed at the Microscopy & Imaging Shared Resource of the Georgetown Lombardi Cancer Center. All shared resources were supported by the NIH Grant P30-CA51008.

Compliance with ethical standards

Conflict of interest TMEM33 (alias SHINC-3) is a Georgetown University patented technology, "Gene SHINC-3 and Diagnostic and Therapeutic Uses Thereof," US Patent # 7244565. IS and UK are co-inventors of this technology. RH, LJ and RC declare that they have no conflict of interest.

Ethical standards The authors declare that all experiments reported in this manuscript were performed in compliance with all current laws and regulations of the United States of America.

References

1. Braakman I, Bulleid NJ (2011) Protein folding and modification in the mammalian endoplasmic reticulum. Ann Rev Biochem 80:71–99
2. Brodsky JL (2012) ERAD-cleaning up: ER-associated degradation to the rescue. Cell 151:1163–1167
3. Hetz C, Chevet E, Harding HP (2013) Targeting the unfolded protein response in disease. Nat Rev Drug Discov 12:703–719
4. Villeneuve NF, Tian W, Wu T, Sun Z, Lau A, Chapman E et al (2013) USP15 negatively regulates Nrf2 through deubiquitination of Keap1. Mol Cell 51:68–79
5. Chitnis NS, Pytel D, Bobrovnikova-Marjon E, Pant D, Zheng H, Maas NL et al (2012) miR-211 is a prosurvival microRNA that regulates Chop expression in a PERK-dependent manner. Mol Cell 48:353–364
6. Tabas I, Ron D (2011) Integrating the mechanisms of apoptosis induced by endoplasmic reticulum stress. Nat Cell Biol 13:184–190
7. Rao RV, Hermel E, Castro-Obregon S, del Rio G, Ellerby LM, Ellerby HM et al (2001) Coupling endoplasmic reticulum stress to the cell death program. Mechanism of caspase activation. J Biol Chem 276:33869–33874
8. Lépine S, Allegood JC, Park M, Dent P, Milstien S, Spiegel S (2011) Sphingosine-1-phosphate phosphohydrolase-1 regulates ER stress-induced autophagy. Cell Death Differ 18:350–361
9. Gewirtz DA (2014) The four faces of autophagy: implications for cancer therapy. Can Res 74:647–651
10. Lamb CA, Yoshimori T, Tooze SA (2013) The autophagosome: origins unknown, biogenesis complex. Nat Rev Mol Cell Biol 14:759–774
11. Denoyelle C, Abou-Rjaily G, Bezrookove V, Verhaegen M, Johnson TM, Fullen DR et al (2006) Anti-oncogenic role of the endoplasmic reticulum differentially activated by mutations in the MAPK pathway. Nat Cell Biol 8:1053–1063
12. Avivar-Valderas A, Wen HC, Aguirre-Ghiso JA (2014) Stress signaling and the shaping of the mammary tissue in development and cancer. Oncogene 33:5483–5490
13. Hart LS, Cunningham JT, Datta T, Dey S, Tameire F, Lehman SL et al (2012) ER stress-mediated autophagy promotes Myc-dependent transformation and tumor growth. J Clin Investig 122:4621–4634
14. Shajahan-Haq AN, Cook KL, Schwartz-Roberts JL, Eltayeb AE, Demas DM, Warri AM et al (2014) MYC regulates the unfolded protein response and glucose and glutamine uptake in endocrine resistant breast cancer. Mol Cancer. doi:10.1186/1476-4598-13-239
15. Brünner N, Boulay V, Fojo A, Freter CE, Lippman ME, Clarke R (1993) Acquisition of hormone-independent growth in MCF-7 cells is accompanied by increased expression of estrogen-regulated genes but without detectable DNA amplifications. Cancer Res 53:283–290
16. Brünner N, Boysen B, Jirus S, Skaar TC, Holst-Hansen C, Lippman J et al (1997) MCF7/LCC9: an antiestrogen-resistant MCF-7 variant in which acquired resistance to the steroidal antiestrogen ICI 182,780 confers an early cross-resistance to the nonsteroidal antiestrogen tamoxifen. Cancer Res 57:3486–3493
17. Butler WB, Fontana JA (1992) Responses to retinoic acid of tamoxifen-sensitive and—resistant sublines of human breast cancer cell line MCF-7. Cancer Res 52:6164–6167
18. Boudreau HE, Broustas CG, Gokhale PC, Kumar D, Mewani RR, Rone JD et al (2007) Expression of BRCC3, a novel cell cycle regulated molecule, is associated with increased phospho-ERK and cell proliferation. Int J Mol Med 19:29–39
19. Broustas CG, Ross JS, Yang Q, Sheehan CE, Riggins R, Noone AM et al (2010) The proapoptotic molecule BLID interacts with Bcl-XL and its downregulation in breast cancer correlates with poor disease-free and overall survival. Clin Cancer Res 16:2939–2948
20. Broustas CG, Grammatikakis N, Eto M, Dent P, Brautigan DL, Kasid U (2002) Phosphorylation of the myosin-binding subunit of myosin phosphatase by Raf-1 and inhibition of phosphatase activity. J Biol Chem 277:3053–3059
21. The National Center for Biotechnology Information Database (2015) http://www.ncbi.nlm.nih.gov. Accessed 21 April 2015
22. The SIB Bioinformatics Resource Portal (2015) http://web.ExPASy.org. Accessed 21 April 2015
23. The UniProt Datasbase (2015) http://www.uniprot.org/uniprot/P57088. Accessed 21 April 2015
24. The PhosphoSitePlus Database (2015) http://www.phosphosite.org. Accessed 21 April 2015
25. The PSORT WWW-Server (2007) http://psort.ims.u-tokyo.ac.jp. Accessed 26 July 2007
26. TOPO2 Transmembrane Protein Image Display Form (2015) http://www.sacs.ucsf.edu/cgi-bin/open-topo2.py. Accessed 21 April 2015
27. Phobius A Combined Transmembrane Topology and Signal Peptide Predictor (2015) http://www.phobius.sbc.su.se/cgi-bin/predict.pl. Accessed 21 April 2015
28. The *cBioPortal* for Cancer Genomics (2015) http://www.cbioportal.org/cross_cancer.do?tab_index=tab_visualize&cancer_study_id=all&gene_list=TMEM33&data_priority=0&Action=Submit#crosscancer/overview/0/TMEM33. Accessed 21 April 2015
29. Gao J, Aksoy BA, Dogrusoz U, Dresdner G, Gross B, Sumer SO et al (2013) Integrative analysis of complex cancer genomics and clinical profiles using the cBioPortal. Sci Signal 6:pl1. doi:10.1126/scisignal.2004088
30. Cerami E, Gao J, Dogrusoz U, Gross BE, Sumer SO, Aksoy BA et al (2012) The cBio cancer genomics portal: an open platform for exploring multidimensional cancer genomics data. Cancer Discov 2:401–404
31. Gomez BP, Riggins RB, Shajahan AN, Klimach U, Wang A, Crawford AC et al (2007) Human X-box binding protein-1 confers both estrogen independence and antiestrogen resistance in breast cancer cell lines. FASEB J 21:4013–4027
32. Clarke R, Shajahan AN, Riggins RB, Cho Y, Crawford A, Xuan J et al (2009) Gene network signaling in hormone responsiveness modifies apoptosis and autophagy in breast cancer cells. J Steroid Biochem Mol Biol 114:8–20
33. Clarke R, Cook KL, Hu R, Facey CO, Tavassoly I, Schwartz JL et al (2012) Endoplasmic reticulum stress, the unfolded protein response, autophagy, and the integrated regulation of breast cancer cell fate. Cancer Res 72:1321–1331
34. Loi S, Haibe-Kains B, Desmedt C, Lallemand F, Tutt AM, Gillet C et al (2007) Definition of clinically distinct molecular subtypes in estrogen receptor-positive breast carcinomas through genomic grade. J Clin Oncol 25:1239–1246

35. Loi S, Haibe-Kains B, Desmedt C, Wirapati P, Lallemand F, Tutt AM et al (2008) Predicting prognosis using molecular profiling in estrogen receptor-positive breast cancer treated with tamoxifen. BMC Genom. doi:10.1186/1471-2164-9-239
36. Loi S, Haibe-Kains B, Majjaj S, Lallemand F, Durbecq V, Larsimont D et al (2010) PIK3CA mutations associated with gene signature of low mTORC1 signaling and better outcomes in estrogen receptor-positive breast cancer. Proc Natl Acad Sci USA 107:10208–10213
37. Zhang Y, Sieuwerts AM, McGreevy M, Casey G, Cufer T, Paradiso A et al (2009) The 76-gene signature defines high-risk patients that benefit from adjuvant tamoxifen therapy. Breast Cancer Res Treat 116:303–309
38. Rigbolt KT, Prokhorova TA, Akimov V, Henningsen J, Johansen PT, Kratchmarova I et al (2011) System-wide temporal characterization of the proteome and phosphoproteome of human embryonic stem cell differentiation. Sci Signal 4:rs3
39. Kim W, Bennett EJ, Huttlin EL, Guo A, Li J, Possemato A et al (2011) Systematic and quantitative assessment of the ubiquitin-modified proteome. Mol Cell 44:325–340
40. Wagner SA, Beli P, Weinert BT, Nielsen ML, Cox J, Mann M et al (2011) A proteome-wide, quantitative survey of in vivo ubiquitylation sites reveals widespread regulatory roles. Mol Cell Proteomics 10:M111
41. STRING: Functional Protein Association Networks (2015) http://string905.embl.de/newstring_cgi/show_network_section.pl?taskId=ICWNuYf_Ewcx&interactive=no&advanced_menu=yes&network_flavor=evidence. Accessed 21 April 2015
42. Avivar-Valderas A, Salas E, Bobrovnikova-Marjon E, Diehl JA, Nagi C, Debnath J et al (2011) PERK integrates autophagy and oxidative stress responses to promote survival during extracellular matrix detachment. Mol Cell Biol 31:3616–3629
43. BLAST: Basic Local Alignment Search Tool (2015) http://www.blast.ncbi.nlm.nih.gov/Blast.cgi. Accessed 21 April 2015